Appendix A

MATLAB CODES

This section provides some of the important Matlab source codes written during the course of this research. Most of the codes written are for the plots and graphs of the theoretical expressions and experimental data in this work.

Spot size against V-number

The spot size of a can be estimated from the fiber core radius *a* and the V-number based on Marcuse's equation [1].

$$\frac{\omega}{a} = 0.65 + \frac{1.619}{V^{3/2}} + \frac{2.879}{V^{6}} \tag{A.1}$$

$$V = \frac{2\pi a}{\lambda} NA \tag{A.2}$$

where *NA* is the numerical aperture, λ is the wavelength and ω is the spot radius.

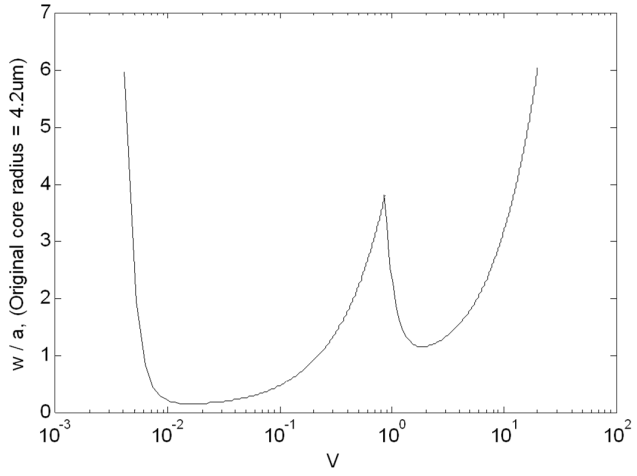

Figure A.1: The graph of absolute spot size against V-number

Code:

```
clear all;
lambda = 1.55e-6;
NA_co = 0.13;
NA_cl = 1.042;
a_cl = 125e-6/2;
a_co = 8.4e-6/2;
k = a_cl/a_co;
h = k*NA_cl/NA_co;
V = linspace(0.86,20,500);
w = lambda/(2*pi*NA_co*a_co)*V.*(0.65+1.619*V.^-1.5 + ...
    2.879*V.^-6);
semilogx(V,w);
clear w;
V = linspace(4.1e-3,0.86,800);
w = lambda*h/(2*pi*NA_cl*a_co)*V.* ...
    (0.65+1.619*(h*V).^-1.5 + 2.879*(h*V).^-6);
hold on
semilogx(V,w)
hold off
xlabel('V_c_o_r_e');
ylabel('w / a_c_o_r_e, (Untapered a_c_o_r_e= 4.2um)');
```

Transmission Spectrum of Self-touching Loop Resonator

Both MLR and MKR self-touching loop resonator and they share the same optical properties; the same transmission equation as shown below [2] can be used to describe both structures.

$$|T|^2 = \left| \frac{e^{-\alpha L/2} e^{j\beta L} - \sin K}{1 - e^{-\alpha L/2} e^{j\beta L} \sin K} \right|^2 \qquad \text{(A.3)}$$

where $\beta = \frac{2\pi n_{eff}}{\lambda}$, α is the attenuation constant, L is the round-trip length and sin$K$ is the amplitude coupling ratio.

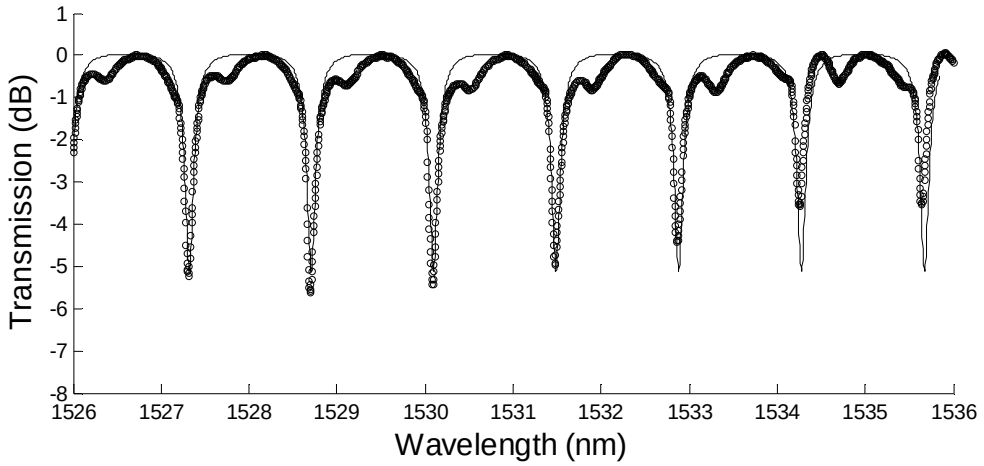

Figure A.2: A typical transmission spectrum of an MKR. The experimental data (circles) with its best-fit theoretical curve.

Code:

```
clear all;
clc;
lam = xlsread('compile.xlsx','Sheet2','A2:A2002');
I = xlsread('compile.xlsx','Sheet2','BW2:BW2002');
lam2_offset = -0.15;
lam2 = linspace(min(lam),max(lam),2001);
lambda = lam2*1e-9;
n = 1.44;
beta = 2*pi*n./lambda;
alpha = 140;L = 1.17e-3;
Kr = asin(exp(-alpha*L/2));
K = 0.73*Kr;
sig = exp(-alpha*L/2);
T = exp((-alpha/2+i*beta).*L)-sin(K);
T = T./(1-sin(K).*exp((-alpha/2+i*beta).*L));
S_offset = 0.13;
S = 10*log10(abs(T).^2)+S_offset;
figure('Position',[ 100 200 700 300])
hold on
plot(lam2+lam2_offset,S,'k-');
hold off
hold on
plot(lam, I, 'ko','MarkerSize',4);
hold off
xlabel('Wavelength (nm)','FontSize',14)
ylabel('Transmission (dB)','FontSize',14)
xlim([1526 1536]);
ylim([-8 1]);
clear all;
clc;
lam = xlsread('compile.xlsx','Sheet2','A2:A2002');
I = xlsread('compile.xlsx','Sheet2','BW2:BW2002');
lam2_offset = -0.15;
lam2 = linspace(min(lam),max(lam),2001);
lambda = lam2*1e-9;
n = 1.44;
beta = 2*pi*n./lambda;
alpha = 140;L = 1.17e-3;
```

```
Kr = asin(exp(-alpha*L/2));
K = 0.73*Kr;
sig = exp(-alpha*L/2);
T = exp((-alpha/2+i*beta).*L)-sin(K);
T = T./(1-sin(K).*exp((-alpha/2+i*beta).*L));
S_offset = 0.13;
S = 10*log10(abs(T).^2)+S_offset;
figure('Position',[ 100 200 700 300])
hold on
plot(lam2+lam2_offset,S,'k-');
hold off
hold on
plot(lam, I, 'ko','MarkerSize',4);
hold off
xlabel('Wavelength (nm)','FontSize',14)
ylabel('Transmission (dB)','FontSize',14)
xlim([1526 1536]);
ylim([-8 1]);
```

Transmission Spectrum of Microfiber Mach-Zehnder Interferometer

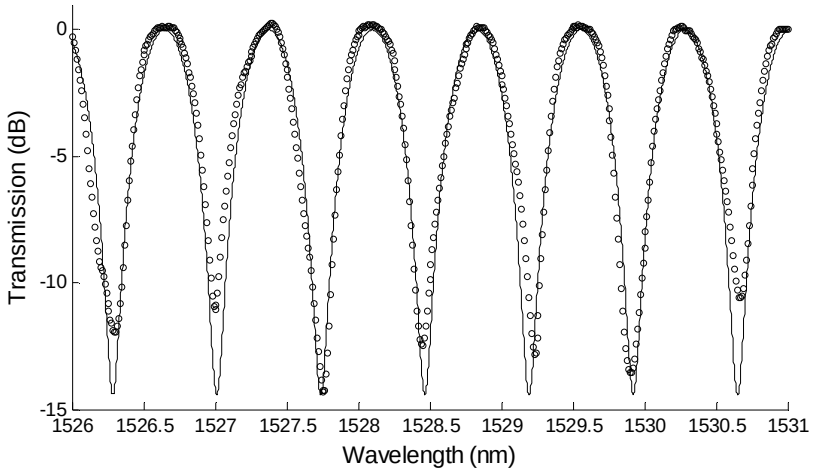

Figure A.3: A typical transmission spectrum of an MMZI. The experimental data (circles) with its best-fit theoretical curve.

Transfer function of the MMZI is given by

$$|T|^2 = a + b\cos\beta\Delta L \qquad \text{(A.4)}$$

where $\beta = \frac{2\pi n_{eff}}{\lambda}$, ΔL is the path length difference, a and b are arbitrary constants and

$a, b > 0$.

Code:

```
clear all;
clc;
x = xlsread('Book1.xls','Sheet4','A2:C2002');
lam = x(1:1:2001,1);
I = x(1:1:2001,3);
lam2 = linspace(min(lam),max(lam),10000);
lambda = lam2*1e-9;
n = 1.44;
beta = 2*pi*n./lambda;
L= 2.23e-3;
phi= 2.7;
a = 0.518;
b =0.482;
S = a+b.*cos(-beta*L + phi);
S = 10*log10(S);
hold on
plot(lam2,S,'k-');
hold off
hold on
plot(lam, I, 'ko','MarkerSize',4);
hold off
xlabel('Wavelength (nm)')
ylabel('Transmission (dB)')
xlim([1526 1531]);
ylim([-15 1]);
```

Reference

[1] D. Marcuse, "Loss analysis of single-mode fiber splices," *Bell Syst. Tech. J.*, vol. 56, no., p. 703, 1977.

[2] M. Sumetsky, Y. Dulashko, J. M. Fini, A. Hale, and D. J. DiGiovanni, "The microfiber loop resonator: theory, experiment, and application," *Lightwave Technology, Journal of*, vol. 24, no. 1, pp. 242-250, 2006.

Appendix B

LIST OF PUBLICATIONS

Journal

Journal

1. S. W. Harun, **K. S. Lim**, A. A. Jasim, and H. Ahmad, "Dual wavelength erbium-doped fiber laser using a tapered fiber," Journal of Modern Optics, vol. 57, no. 21, pp. 2111-2113, 2010.
2. S. W. Harun, **K. S. Lim**, A. A. Jasim, and H. Ahmad, "Fabrication of Tapered Fiber Based Ring Resonator," Laser Physics, vol. 20, no. 7, pp. 1629-1631, 2010.
3. S. W. Harun, H. Z. Yang, **K. S. Lim**, M. R. Tamjis, K. Dimyati, and H. Ahmad, "Fiber optic displacement sensor based on concave mirror," Optoelectronics and Advanced Materials-Rapid Communications, vol. 3, no. 11, pp. 1139-1141, 2009.
4. **K. S. Lim**, S. W. Harun, H. Z. Yang, K. Dimyati, and H. Ahmad, "Analytical and experimental studies on asymmetric bundle fiber displacement sensors," Journal of Modern Optics, vol. 56, no. 17, pp. 1838-1842, 2009.
5. **K. S. Lim**, M. R. A. Moghaddam, S. W. Harun, and H. Ahmad, "Tunable-Spacing Multi-wavelength Yb-Doped Fiber Laser (YDFL) Based on Temperature Sensitive Loop Mirror," Lasers in Engineering, vol. 20, no. 1-2, pp. 39-45, 2010.
6. **K. S. Lim**, C. H. Pua, S. W. Harun, and H. Ahmad, "Temperature-sensitive dual-segment polarization maintaining fiber Sagnac loop mirror," Optics and Laser Technology, vol. 42, no. 2, pp. 377-381, 2010.

7. M. R. A. Moghaddam, S. W. Harun, S. Shahi, **K. S. Lim**, and H. Ahmad, "Comparisons of Multi-Wavelength Oscillations Using Sagnac Loop Mirror and Mach-Zehnder Interferometer for Ytterbium Doped Fiber Lasers," Laser Physics, vol. 20, no. 2, pp. 516-521, 2010.

8. S. Shahi, S. W. Harun, **K. S. Lim**, A. W. Naji, and H. Ahmad, "Enhanced Four-Wave Mixing Efficiency Of Bi-EDF In A New Ring Configuration For Determination of Nonlinear Parameters," Journal of Electromagnetic Waves and Applications, vol. 23, no. 17-18, pp. 2397-2407, 2009.

9. H. Z. Yang, **K. S. Lim**, S. W. Harun, K. Dimyati, and H. Ahmad, "Enhanced bundle fiber displacement sensor based on concave mirror," Sensors and Actuators a-Physical, vol. 162, no. 1, pp. 8-12, 2010.

10. S. W. Harun, **K. S. Lim**, S. S. A. Damanhuri, H. Ahmad, "Microfiber loop resonator based temperature sensor", J. Europ. Opt. Soc. Rap. Public., vol 6, no. 11026, 2011.

11. **K. S. Lim**, S. W. Harun, S. S. A. Damanhuri, A. A. Jasim, C. K. Tio, and H. Ahmad, "Current sensor based on microfiber knot resonator," Sensors and Actuators A: Physical, vol. 167, no. 1, pp. 377–381, 2011.

12. **K. S. Lim**, C. H. Pua, N. A. Awang, S. W. Harun and H. Ahmad, Fiber loop mirror filter with two-stage high birefringence fibers, Progress In Electromagnetics Research C, Vol. 9, pp. 101-108, 2009.

13. **K. S. Lim**, S. W. Harun, A. A. Jasim, and H. Ahmad, "Fabrication of microfiber loop resonator-based comb filter," Microwave and Optical Technology Letters, vol. 53, no. 5, pp. 1119-1121, 2011.

14. **K. S. Lim**, A. A. Jasim, S. S. A. Damanhuri, S. W. Harun, B. M. A. Rahman, and H. Ahmad, "Resonance Condition of Microfiber Knot Resonator Immersed in Liquids," Applied Optics, vol. 50, no. 29, pp. 5912-5916, 2011

15. **K. S. Lim**, S.W. Harun, S. S. A. Damanhuri, A. A. Jasim, H. H. Ku, and H. Ahmad, "Low cost Spectral Tunable Microfiber Knot Resonator," IET Optoelectronics, vol. 5, no. 6, pp.281–284, 2011.

16. Y. K. Cheong, **K. S. Lim**, W. H. Lim, W. Y. Chong, R. Zakaria, and H. Ahmad, "Fabrication of Tapered Fibre Tip using Mechanical Polishing Method," Review of Scientific Instruments, vol. 82, no. 8, pp. 086115 (3), 2011

17. A. Sulaiman, S.W. Harun, **K.S. Lim**, F. Ahmad, H. Ahmad, "Microfiber Mach-Zehnder interferometer embedded in low index polymer," Optics & Laser Technology, vol. 44, no. 4, pp. 1186–1189, 2011.

18. W. Y. Chong, **K. S. Lim**, W. H. Lim, S. W. Harun, F. R. Mahamd Adikan, H. Ahmad, "Spreading profile of evaporative liquid drops in thin porous layer", Physical Review E, (In press) 2012.

19. H. Ahmad, I. Aryanfar, **K. S. Lim**, W. Y. Chong, S. W. Harun, "Microfiber Mach-Zehnder / Sagnac Interferometer," IEEE Photonic Technology Letter, (Under review) 2012.

20. **K. S. Lim**, S. Yoo, M. C. Paul, H. Ahmad, M. Pal, S. K. Bhadra, and J. K. Sahu, "Tunable laser in Ytterbium doped Y2O3 nanoparticle optical fibers," IEEE Photonic Technology Letter, (Under review) 2012.

Conference

1. S. W. Harun, **K. S. Lim**, A. A. Jasim, and H. Ahmad, "Fabrication of optical comb filter using tapered fiber based ring resonator," Southeast Asian International Advances in Micro/Nanotechnology, vol. 7743, no., 2010.

2. S. Shahi, S. W. Harun, **K. S. Lim**, R. Parvizi, M. R. A. Moghaddam and H. Ahmad, "Application of Four-Wave Mixing For Determination of Nonlinear Parameter Based on Bi-EDF", The 5th Mathematics and Physical Sciences Graduate Congress, 2009.

Sensors and Actuators A xxx (2011) xxx–xxx

Contents lists available at ScienceDirect

Sensors and Actuators A: Physical

journal homepage: www.elsevier.com/locate/sna

Current sensor based on microfiber knot resonator

K.S. Lim [a], S.W. Harun [a,b,*], S.S.A. Damanhuri [b], A.A. Jasim [b], C.K. Tio [b], H. Ahmad [a]

[a] Photonics Research Center, Department of Physics, University of Malaya, 50603 Kuala Lumpur, Malaysia
[b] Department of Electrical Engineering, University of Malaya, 50603 Kuala Lumpur, Malaysia

ARTICLE INFO

Article history:
Received 24 November 2010
Received in revised form 8 February 2011
Accepted 17 February 2011
Available online xxx

Keywords:
Wavelength tunability
Current sensor
Microfiber knot resonator

ABSTRACT

A compact current sensor using a microfiber knot resonator (MKR) is demonstrated. With the assistance of a copper wire that is wrapped by the microfiber knot, resonant wavelength inside the MKR can be tuned by applying electric current to the copper wire. The resonant wavelength change is based on the thermally induced optical phase shift in the MKR due to the heat produced by the flow of electric current over a short transit length. It is shown that the wavelength shift is linearly proportional to the square of the amount of current and the maximum tuning slope of 51.3 pm/A^2 is achieved using a newly fabricated MKR.

1. Introduction

Microfibers/nanofibers have attracted growing interest recently especially in their fabrication methods and applications. This is due to a number of interesting optical properties of these devices, which can be used to develop low-cost, miniaturized and all-fiber based optical devices for various applications [1,2]. For instance, many research efforts have focused on the development of microfiber/nanofiber based optical resonators that can serve as optical filters, which have many potential applications in optical communication and sensors [3]. Of late, many microfiber structures have been reported such as microfiber loop resonator (MLR) [3,4], microfiber coil resonator (MCR) [5,6], microfiber knot resonator (MKR) [7,8], and reef knot microfiber resonator as an add/drop filter [9]. These devices are very sensitive to a change in the surrounding refractive index due to the large evanescent field that propagates inside the fiber and thus they can find many applications in various optical sensors.

A variety of fiber optic based current sensors have been investigated in recent years using mainly a single mode fiber (SMF) of clad silica. They are typically divided into two categories, where one is based on Faraday effect and the other is based on thermal effect. The former is capable of measuring electrical currents remotely, but the device requires a long fiber due to the extremely small Verdet constant of silica. The latter needs only a short length of fiber but requires complex manufacturing techniques to coat the fibers with metals. Recently, a resonant wavelength of the microfiber loop resonator (MLR) has been experimentally reported to shift when electric current is applied to the loop through a copper rod. An acceptable transmission loss is achieved despite the fact that copper is not a good low-index material to support the operation of such structure [1]. This finding has opened up a way to produce dynamic and low cost current sensors by manipulating an electric current dependence spectral shift characteristic of the microfiber based resonator.

In this work, a compact current sensor is demonstrated using the MKR, based on the idea of measuring the thermally induced resonant wavelength shift as a result of heat produced due to the flow of electric current over a copper rod. Experimental and analytical studies on the characteristic of the resonant wavelength of an MKR, which is tied to a copper rod are carried out. To our knowledge, this is the first time such an MKR based current sensor is reported.

2. Theoretical background

MKRs share most of the optical properties of MLRs such as the free spectral range, which can be expressed as;

$$\mathrm{FSR} \approx \frac{\lambda^2}{n_{eff} L} \tag{1}$$

where λ is the operating wavelength, n_{eff} is the effective index of the microfiber and L denotes the single roundtrip length in the resonator. The temperature variation affects both effective refractive index, n_{eff} and the loop length L, of the MKR. The variation in both parameters may lead to spectral shift and the relationship can be

* Corresponding author at: Department of Electrical Engineering, University of Malaya, 50603 Kuala Lumpur, Malaysia.
E-mail address: swharun@um.edu.my (S.W. Harun).

0924-4247/$ – see front matter © 2011 Elsevier B.V. All rights reserved.
doi:10.1016/j.sna.2011.02.036

expressed as;

$$\frac{\Delta\lambda_{res}}{\lambda_{res}} = \left(\frac{\Delta n_{eff}}{n_{eff}} + \frac{\Delta L}{L}\right)_{Temp.} \quad (2)$$

Each term on the right hand side of Eq. (2) can be expressed in linear forms with temperature change ΔT as shown below:

$$\frac{\Delta n}{n} = \alpha\Delta T \quad (3)$$

$$\frac{\Delta L}{L} = \beta\Delta T \quad (4)$$

where α and β are the thermal expansion coefficient (TEC) and thermal-optic coefficient (TOC) of the microfibers, respectively [8]. From the dimensionless fractional term $\Delta L/L$ in Eq. (4), it is easily understood that at a given temperature change, the same resonant wavelength shift of the MKR can be achieved for any loop length value, L. By applying current, the copper rod acts as a heating element and the heat generated leads to instantaneous temperature rise in the MKR. Consider the linear relationship between the temperature change and heat energy generated by the conducting current. The relationship between the wavelength shift and the conducting current, I can be expressed in the form of

$$\frac{\Delta\lambda_{res}}{\lambda_{res}} \propto \frac{\rho I^2}{A} \quad (5)$$

where ρ and A represent the conductor resistivity and the cross-sectional area of the conductor rod, respectively. The term ρ/A in Eq. (5) is equivalent to the resistance per unit length of the conductor material. The resistivity of the copper rod is $1.68 \times 10^{-8}\ \Omega$ m.

3. Fabrication of microfiber knot resonator

At first, a microfiber is fabricated from a silica-based single mode fiber (SMF) using a flame-brushing method [10]. After the polymer protective cladding has been removed from a piece of SMF, a tapered fiber is made by heating and stretching the SMF until ~2 μm waist diameter is acquired. Then the microfiber is cut and separated into two unequal parts in which the longer one is used in the knot fabrication and the other part is used as a collector fiber to collect the transmitted light from the MKR [5]. The microfiber knot is assembled by micromanipulation of the longer part of the microfiber, which has a high diameter uniformity and excellent sidewall smoothness. The microfiber is first twisted into a relatively large loop, which is slightly larger than the diameter of the copper wire. The copper wire is inserted into the loop, which is then tightened onto the copper wire by pulling the free ends of the fiber as illustrated in Fig. 1. Another part of microfiber (the collection fiber) is used to collect the light transmitted out from the knot by means of evanescent coupling. At least ~3 mm of coupling length between two microfibers is required to achieve strong Van der Waal attraction force to keep them attached together as shown in Fig. 1. The wire diameter is measured to be approximately 185 μm.

The knot configuration is sustained by elastic-bend-induced tensile force and friction at the intertwisted area. The optical characteristics of the resonator are easily affected by the tensile strain produced during the pulling and tightening process. It is essential to relax the tension on both arms of the MKR by moving the fiber holders a bit closer to the microfiber knot after the knot is fastened. In spite of a very little change at the knot size, the resonance condition of the MKR remains good and stable after the tension is released. Unlike microfiber loop resonator, the elastic-bend-induced tensile force and friction at the intertwisted area offers higher structural stability to ensure strong contact at the coupling region and maintain a consistent resonance condition of the resonator [6].

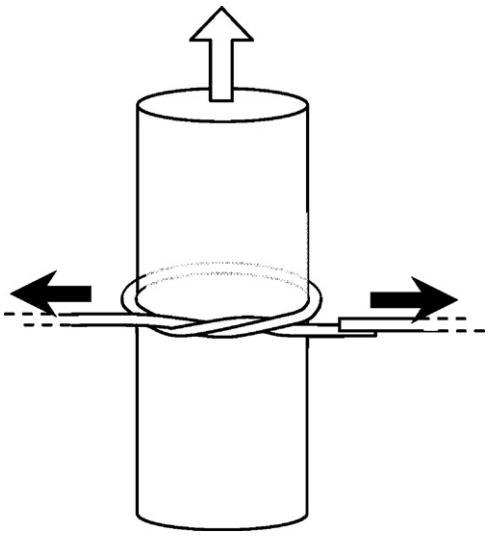

Fig. 1. Schematic illustration of MKR tied on a copper rod. The upward arrow in the figure indicates the direction of the electric current in the copper rod.

4. Results and discussion

For optical characterization of the MKR, broadband source from amplified spontaneous emission is first launched into and guided along the SMF and then squeezed into the microfiber through the taper area. The light transmitted out from the MKR is collected by the collection fiber and measured by an optical spectrum analyzer (OSA). The optical resonance is generated when light traversing the MKR acquires a phase shift multiple of 2π When an alternating current flows through the copper wire, heat is produced in the wire causing temperature to change. Since the MKR is in contact with the copper wire, any temperature changes will influence the refractive index and the optical path length of the MKR.

Fig. 2 shows the resonant spectra of the MKR tied on a copper wire with various current loadings. In the experiment, the applied current is uniformly increased from 0 to 2 A. As shown in Fig. 2, the resonant wavelength shifts to a longer wavelength with the increase in conducting current of the copper wire. The response time of the wavelength shift is approximately 3 s and the spectrum comes to a steady condition after 8 s. Therefore, each spectrum is recorded at ~10 s after the copper wire is loaded with an electric current. At loading current I = 1.0 A, the resonant wavelength is shifted by ~30 pm from 1530.56 nm to 1530.59 nm and at I = 2.0 A, the resonant wavelength is further shifted to 1530.77 nm, 210 pm from the original wavelength. Inset of Fig. 2 shows the free spectral range of the transmitted spectrum against the applied currents. As shown in the inset, FSR of the MKR remains unchanged at 1.5 nm

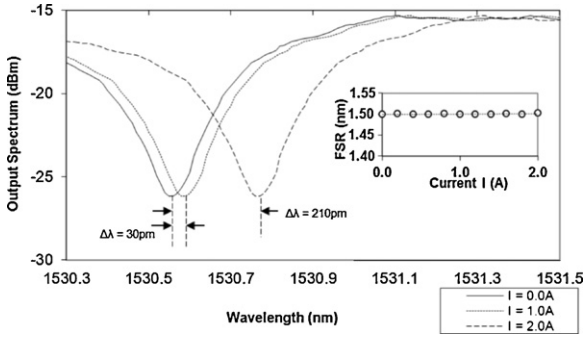

Fig. 2. Resonant wavelength shift of the MKR tied on a copper rod loaded with different currents. Inset shows unchanged FSR with the increasing current.

Please cite this article in press as: K.S. Lim, et al., Current sensor based on microfiber knot resonator, Sens. Actuators A: Phys. (2011), doi:10.1016/j.sna.2011.02.036

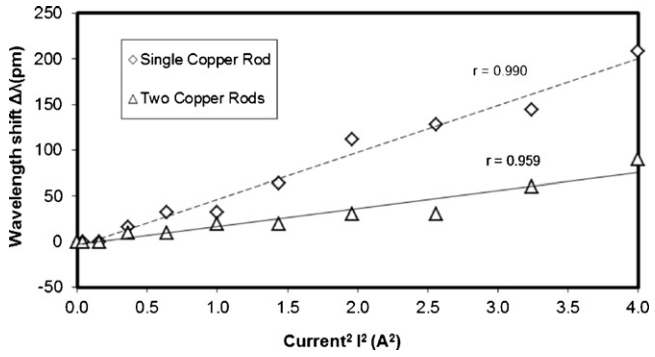

Fig. 3. Current response of MKRs based on single-wire and two-wire configurations. The calculated resistance of the single copper wire and two copper wire are 0.53 Ω m^{-1} and 0.26 Ω m^{-1}, respectively.

with the increasing current. The calculated *Q* factor and finesse of the MKR are ~4400 and 4.3, respectively. It is also observed that the transmission spectrum always shift towards the longer wavelength direction with increasing current regardless of the current flow direction, and the spectrum returns to the original state once current supply is terminated.

The experiment is also repeated for the use of two copper rods for comparison purpose. In this case, the MKR is tightened onto two copper wires with identical wire diameter. The measured FSR and knot diameter of the MKR with two-wire are 1.5 nm and ~370 μm 1.7 nm, respectively. An alternating current flows through the copper wire and the resonant wavelength shift is investigated against the applied current for both cases; single- and two-wire arrangements. At a small current of <0.5 A, no significant resonant wavelength shift is observed. Starting from 0.6 A, the resonant wavelength shifts gradually toward the longer wavelength. At 2.0 A, a wavelength shift of 0.208 nm and 0.09 nm are achieved with single and two copper wires configurations, respectively. Fig. 3 shows the resonant wavelength shift against the square of current (I^2) for both configurations. The data set of each configuration can be well fitted to a linear regression line with a correlation coefficient value of $r > 0.95$. This justifies the linear relationship stated in Eq. (5). In comparing the conductor wire cross-sectional area between the two configurations, the two-wire configuration is twice as large as the single-wire configuration. Based on the relation in Eq (5), the tuning slope of the wavelength shift against I^2 of the two-wire configuration should be half of the single-wire configuration. The slope of each line is 51.3 pm/A^2 (single rod) and 19.5 pm/A^2 (two rods) nonetheless it is reasonable to attribute the mismatch between the analysis and experiment to the different orientation and position of the rod(s) in the MKR.

In an earlier work, Guo et al. [1] demonstrated that the wavelength shift of MLR increases linearly with the increase of the electric current with a slope of 26.5 pm/A. At lower loading current, the current response of wavelength shift is very small and it is very close to linear relationship with increasing current (pm/A). However, this relation does not hold as the loading current goes higher. The results in this work indicate that the wavelength shift is proportional to the square of electric current, with a slope dimension of pm/A^2. Besides, MKR offers several advantages if compared with MLR for instance better coupling efficiency in the resonator due to the small coupling width between microfibers in the structure, no external force on the microfiber is required to achieve stable wrapping of microfiber on the copper wire. The tuning slope of the current sensor can be further increased if conductors with higher resistivity are used such as nichrome, constantan, and graphite. which are commonly used as heating elements. However, the suitability of the elements when integrated with the microfiber or other opto-dielectric device requires further investigation.

5. Conclusion

A compact current sensor is demonstrated using an MKR which is obtained from manipulating freestanding silica microfiber. With the assistance of a copper wire that is wrapped by the microfiber knot, resonant wavelength inside the MKR can be tuned by applying electric current to the copper wire. The wavelength shift is due to the thermally induced optical phase shifts attributable to the heat produced by the flow of current. The theoretical and experimental analysis suggests that the tuning slope of the MKR can be manipulated by using different cross-sectional area and resistivity of the conductor rod. It is shown experimentally that the wavelength shift is linearly proportional to square of the amount of current. The tuning slope of 51.3 pm/A^2 based on a single copper wire configuration has also been demonstrated.

References

[1] X. Guo, Y. Li, X. Jiang, L. Tong, Demonstration of critical coupling in microfiber loops wrapped around a copper rod, Applied Physics Letters 91 (7) (2007) 073512–173512-3.
[2] S.W. Harun, K.S. Lim, A.A. Jasim, H. Ahmad, Dual wavelength erbium-doped fiber laser using a tapered fiber, Journal of Modern Optics (2010) 1362–3044.
[3] M. Sumetsky, Y. Dulashko, J.M. Fini, A. Hale, D.J. DiGiovanni, The microfiber loop resonator: theory, experiment, and application, Journal of Lightwave Technology 24 (1) (2006) 242–250.
[4] S.W. Harun, K.S. Lim, A.A. Jasim, H. Ahmad, Fabrication of tapered fiber based ring resonator, Laser Physics 20 (7) (2010) 1629–1631.
[5] M. Sumetsky, Basic elements for microfiber photonics: micro/nanofibers and microfiber coil resonators, Journal of Lightwave Technology 26 (2008) 21–27.
[6] F. Xu, G. Brambilla, Embedding optical microfiber coil resonators in Teflon, Optics Letter 32 (15) (2007) 2164–2166.
[7] X. Jiang, L. Tong, G. Vienne, X. Guo, A. Tsao, Q. Yang, D. Yang, Demonstration of optical microfiber knot resonators, Applied Physics Letters 88 (22) (2006) 223501–1223501-3.
[8] Y. Wu, Y. Rao, Y. Chen, Y. Gong, Miniature fiber-optic temperature sensors based on silica/polymer microfiber knot resonators, Optics Express 17 (2009) 18142–18147.
[9] G. Vienne, A. Coillet, P. Grelu, M.E. Amraoui, J. Jules, F. Smektala, L. Tong, Demonstration of a reef knot microfiber resonator, Optics Express 17 (2009) 6224–6229.
[10] G. Brambilla, V. Finazzi, D.J. Richardson, Ultra-low-loss optical fiber nanotapers, Optics Express 12 (2004) 2258–2263.

Biographies

K.S. Lim received his B.E. from the Department of Electrical Engineering, Faculty of Engineering, University of Malaya, Malaysia in 2008. He is currently pursuing his Ph.D. in Photonic Research Center, Department of Physics at the same university. His present research interests are in optics of microfiber resonators, fiber-optic sensors and fiber lasers.

Sulaiman Wadi Harun received the B.E. degree in Electrical and Electronics System Engineering from Nagaoka University of Technology, Japan in 1996, and M.Sc. and Ph.D. degrees in Physics from University of Malaya in 2001 and 2004, respectively. Currently, he is a full professor at the Faculty of Engineering, University of Malaya. His research interests include fiber optic active and passive devices.

S.S.A. Damanhuri received her B.E. in Telecommunication Engineering from Faculty of Engineering, University of Malaya, Malaysia in 2010. She is currently progressing her M.E. in Photonic Research Center, Department of Physics at the same university. Her current field of interests are microfiber resonators and fiber lasers.

A.A. Jasim was born in Baghdad, Iraq on 1 November 1985. He received his B.Sc. in Electrical Engineering from University of Technology-Baghdad in 2007 and M.E. in telecommunication engineering from University of Malaya, Malaysia in 2010. He is currently progressing his Ph.D. program in Photonic Research Center, Department of Physics at the same university. Her current field of interests are nano/microfibers and microfiber photonic devices.

C.K. Tio is current doing his B.E. in the Department of Electrical Engineering, Faculty of Engineering, University of Malaya.

Harith Ahmad received the Ph.D. degree in Laser Technology from the University of Swansea (UK) in 1983. He is a full professor at the Department of Physics, University of Malaya. He is also a fellow member of Malaysian Academic of Science.

Please cite this article in press as: K.S. Lim, et al., Current sensor based on microfiber knot resonator, Sens. Actuators A: Phys. (2011), doi:10.1016/j.sna.2011.02.036

Resonance condition of a microfiber knot resonator immersed in liquids

Kok Sing Lim,[1] Ali A. Jasim,[2] Siti S. A. Damanhuri,[2] Sulaiman W. Harun,[1,2,*] B. M. Azizur Rahman,[3] and Harith Ahmad[1]

[1]Photonics Research Center, Department of Physics, University of Malaya, 50603 Kuala Lumpur, Malaysia

[2]Department of Electrical Engineering, University of Malaya, 50603 Kuala Lumpur, Malaysia

[3]Electrical, Electronic and Information Engineering Department, City University, London, UK

*Corresponding author: swharun@um.edu.my

Received 23 May 2011; revised 19 June 2011; accepted 15 July 2011; posted 15 July 2011 (Doc. ID 147966); published 19 October 2011

Effects of immersing a microfiber knot resonator (MKR) in liquid solutions that have refractive indices close to that of silica are experimentally demonstrated and theoretically analyzed. Significant improvement in resonance extinction ratio within 2 to 10 dB was observed. To achieve a better understanding, a qualitative analysis of the coupling ratio and round-trip attenuation of the MKR is performed by using a curve-fitting method. It was observed that the coupling coefficient at the knot region increased when immersed in liquids. However, depending on the initial state of the coupling and the quantity of the increment in the coupling coefficient when immersed in a liquid, it is possible that the MKR may experience a deficit in the coupling parameter due to the sinusoidal relationship with the coupling coefficient. © 2011 Optical Society of America

OCIS codes: 060.2340, 060.4005, 230.5750.

1. Introduction

Optical microfibers/nanofibers have recently attracted considerable interest as promising building blocks for a wide variety of photonic applications. This is due to their unique optical guidance properties, which include a relatively low loss, strong evanescent fields, tight optical confinement, and controllable waveguide dispersion. Various optical-microfiber-based resonators have also been demonstrated in loop, knot, and coil configurations benefitting from the intrinsic advantages of low scattering/absorption loss, structural simplicity, and direct coupling to input/output fibers. One of the important applications of these resonators is as high-sensitivity optical sensors [1,2], whereby the operating principle normally relies on the characteristics of the resonance. The variations of the positions of the resonance wavelength and extinction ratio of the resonators are significantly dependent on the sensing parameters, such as temperature and refractive index [3,4]. The resonance condition of a resonator also relies on the index contrast between the microfiber and its ambient medium, evanescent field strength, and the distance between the two microfibers in the coupling region.

The large evanescent field that can be found in thinner microfibers is one of the solutions to achieving higher coupling in microfiber resonators. The large fraction of light intensity in the evanescent field allows stronger mode interaction between two microfibers and yields a high coupling coefficient. Caspar and Bachus [5] suggested embedding the microfiber resonator into a medium that has a slightly lower refractive index than that of silica. Because of the small index contrast, the microfiber has a larger evanescent field, which yields stronger coupling in the resonator [5,6]. Besides being used as a postfabrication remedy for improving the resonance condition of the resonator, embedding also offers good protection from the fast aging process and provides

0003-6935/11/305912-05$15.00/0

portability for the microfiber devices. Vienne *et al.* reported that, when a microfiber resonator is embedded in low-index polymer, the optimal resonance wavelength is downshifted by ~20% [7]. However, there are very few reports that provide mathematical analysis on the effect of embedding in low-index contrast medium to the resonance condition of the resonator.

In this paper, we present a mathematical analysis and experimental results on the characteristic of a microfiber knot resonator (MKR) immersed in liquid solutions. This study provides a better understanding of the effect of replacing surrounding air by a liquid. MKR was used in the experiment due to its rigid knot structure and strong interfiber coupling [3]. The knot structure and resonance condition could be easily maintained during the immersing process.

2. Theory

The amplitude transfer function of a self-coupled microfiber resonator can be well defined by the following equation [2]:

$$T = \frac{\exp(-\alpha L/2)\exp(j\beta L) - \sin(K)}{1 - \exp(-\alpha L/2)\exp(j\beta L)\sin(K)}, \tag{1}$$

where α is the intensity attenuation constant, β is the propagation constant along the microfiber, L represents the round-trip length of the resonator, and $\sin(K)$ represents the intensity coupling ratio. K is directly related to the coupling length and it can be expressed as

$$K = \kappa l, \tag{2}$$

where κ is the coupling coefficient and l is the coupling length. For every oscillation in an MKR, the circulating wave undergoes some attenuation in intensity attributed to nonuniformity in the microfiber diameter, material loss, impurity in the ambience of the microfiber, and bending loss along the microfiber loop. These losses can be combined and represented by a round-trip attenuation factor $\exp(-\alpha L/2)$ that is a part of Eq. (1). In the condition when the coupling ratio is equivalent to the round-trip attenuation, a large fraction of the wave power at resonance is annihilated in the oscillation and thus the transmission of the resonance wavelength is minimum [8]. This condition is called critical coupling. The resonance condition is optimal and the resonance extinction ratio (RER) is the highest in this condition. Mathematically, in this condition the numerator of Eq. (1) is equal to zero and, therefore,

$$\sin(K_c) = \exp(-\alpha L/2), \tag{3}$$

where K_c denotes the coupling parameter at critical coupling.

Based on Eq. (1), the resonance transmission amplitude that corresponds to $\beta L = 2m\pi$ is

$$\delta_{\text{res}} = \left|\frac{\exp(-\alpha L/2) - \sin(\kappa l)}{1 - \exp(-\alpha L/2)\sin(\kappa l)}\right|, \tag{4}$$

while the maximum transmission amplitude that occurs at $\beta L = (2m+1)\pi$ is

$$\delta_{\max} = \left|\frac{\exp(-\alpha L/2) + \sin(\kappa l)}{1 + \exp(-\alpha L/2)\sin(\kappa l)}\right|, \tag{5}$$

where m is an integer. RER is given by

$$\text{RER} = 20\log_{10}(\delta_{\max}/\delta_{\text{res}}). \tag{6}$$

In most scenarios, parameters $\sin(\kappa l)$ and $\exp(-\alpha L/2)$ are larger than 0.6 and $|\delta_{\max}| \sim 1$. Therefore, Eq. (6) can be rewritten as

$$\text{RER} \sim 20\log_{10}(\delta_{\text{res}}). \tag{7}$$

A smaller value of δ_{res} indicates that the resonance condition is closer to the critical coupling and it yields a larger value of RER.

3. Experiment and Results

Unlike a microfiber loop resonator (MLR) that exploits van der Waals attractive force to maintain the structure of the loop, an MKR has a more rigid knot structure, with interfiber twisted coupling between microfibers. Nonetheless, each system constitutes a self-coupled loop and they share the same optical properties; Eq. (1) can be used to describe the transmission spectra of both structures. The fabrication of an MKR starts with tapering the fiber using the flame brushing technique [9]. After a 7-cm-long and 3–5-μm-diameter biconical tapered fiber was drawn, it was cut into two parts, where the first part is twice as long as the second. The longer tapered fiber was used for the fabrication of a knot by using tweezers. The shorter section was used as a collector fiber by evanescent coupling with the output port of the knot resonator. After that, the transmission spectrum of the freestanding MKR in air was recorded by an optical spectrum analyzer. Next, the spectrum of the MKR immersed in a propan-2-ol solution that had a refractive index (RI) of 1.37 was measured. First, the MKR was slowly laid horizontally on an earlier prepared flat platform deposited with a thin layer of propan-2-ol. Using a micropipette, a small volume of propan-2-ol solution was dropped onto the MKR to replace the surrounding medium of the MKR with the solution. The structure of the microfiber knot was intact and the resonance was maintained. This is the crucial part that distinguishes an MKR from an MLR. It is very difficult to maintain the loop structure and resonance of an MLR when it is immersed in a liquid solution. Figure 1 shows the microscope image of an ~491 μm knot-diameter MKR immersed in low-index resin. This MKR was assembled from an ~4.5 μm diameter microfiber.

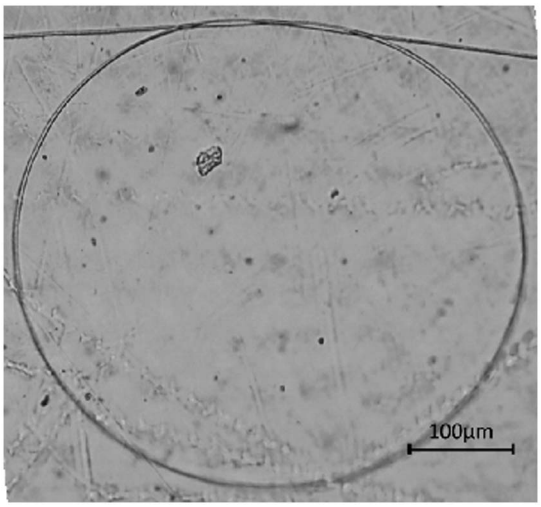

Fig. 1. Optical microscope image of an MKR immersed in low-index resin.

Figure 2 shows the overlaid transmission spectra of the MKR in air (solid) and solution (dashed). Referring to the peak powers of both spectra, it is easy to determine that the MKR had suffered an additional ~7 dB excess loss after it was immersed in the solution. The drop in the coupling efficiency of the output-collector microfiber coupling constitutes a large fraction of this excess loss. This is possibly because of the change in index contrast and the disturbance on the structure of output-collector microfiber coupling when the liquid solution was introduced. In this work, the transmission spectrum of the MKR in the liquid solution was recorded after it was stable. On the other hand, the RER of the MKR improves from ~5 to ~8 dB. It is believed that the structure of the microfiber knot was more rigid than that of output-collector microfiber coupling.

Figures 3(a) and 3(b) show the offset experimental data with their best-fit curves for both experiments in air and solution, respectively, which can be used to analyze the resonance characteristics. The coupling parameter, $\sin(\kappa l)$, and round-trip attenuation factor of MKR, $\exp(-\alpha L/2)$, can be extracted from fitting the curve based on the transfer function in Eq. (1). A trial and error approach is employed in the fitting process until both the experimental and theoretical curves agree with each other. In the air, the best-fit

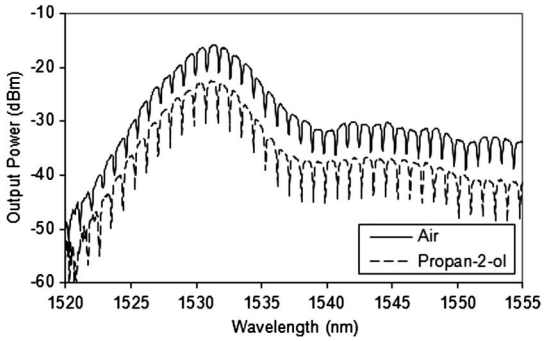

Fig. 2. The transmission spectra of the MKR in the (solid curve) and propan-2-ol solution (dashed curve).

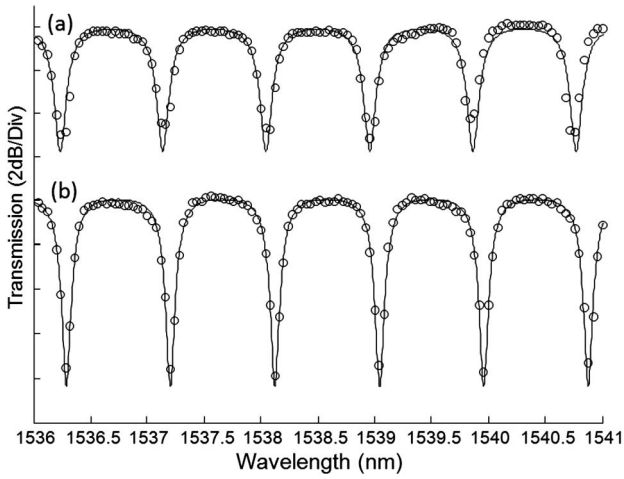

Fig. 3. Offset experimental data (circles) with its best-fit curve (solid curve): (a) air, RI ~ 1.00; (b) propan-2-ol, RI ~ 1.37.

parameters for the transmission spectrum in Fig. 3(a) are $\sin(\kappa l) = 0.6207$ and $\exp(-\alpha L/2) = 0.8547$. By immersing the MKR in propan-2-ol solution, the best-fit parameters of Fig. 3(b) become $\sin(\kappa l) = 0.6762$ and $\exp(-\alpha L/2) = 0.8361$. The lower round-trip attenuation factor (higher round-trip loss, α) can be attributed to the higher bending loss of the microfiber knot in a medium with smaller index contrast. It is well known that microfiber is susceptible to scattering due to surface roughness. The increased evanescent field amplitude of the microfiber in immersion may aggravate the scattering loss. The loss at the output-collector coupling is excluded from this analysis as it only affects the total output power (position in the vertical axis) and it has already been eliminated in the offset spectrum.

From the comparison between the two spectra of Fig. 3, the transmission spectrum with propan-2-ol has higher coupling and a smaller round-trip attenuation factor, which results in a smaller value of $\delta_{res} = 0.3679$ compared with $\delta_{res} = 0.5060$ obtained from the spectrum for air. This explains the larger RER of the transmission spectrum in Fig. 3(b).

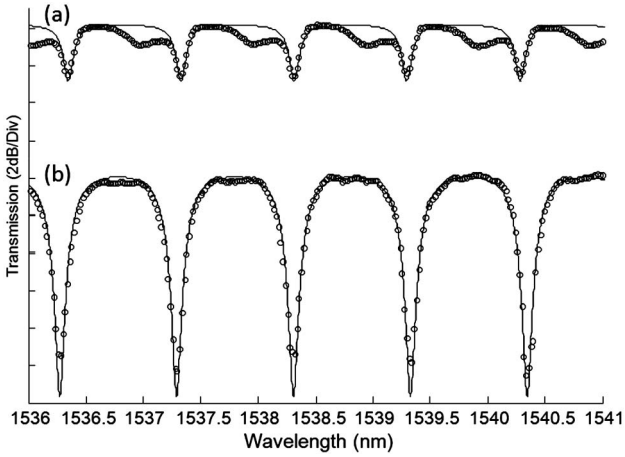

Fig. 4. Transmission spectra of the MKR in different surrounding media: (a) air, RI ~ 1.00; (b) low-index resin, RI ~ 1.36.

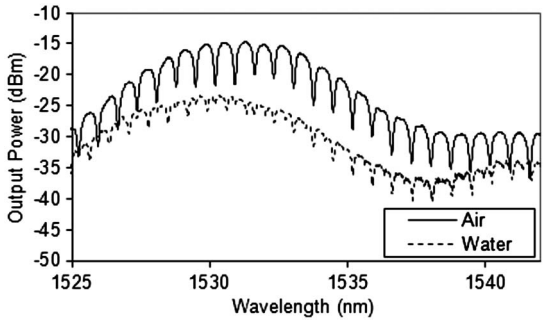

Fig. 5. Example of an MKR with decreased RER after it is immersed in water (RI ~ 1.33).

However, it is also possible that the large increment in the coupling coefficient κ may have forwarded the phase of κl to the next quarter-cycle of the sinusoidal function of $\sin(\kappa l)$) and, thus, produces a lower coupling value. The next experimental data provide an example for such a self-defeating scenario. Figure 4 compares the transmission spectra of an MKR in air and low-index UV-curable resin (UV-Opti-clad 1.36RCM from OPTEM Inc) with an RI of ~1.36. The coupling parameter, $\sin(\kappa l)$ for both spectra is then calculated from the fitting curves. It drops from 0.7132 to 0.6247 when the MKR was immersed in water. On the other hand, the round-trip attenuation factor is also calculated from the fitting and it suffers a greater fall from 0.9432 to 0.7538. In spite of that, the RER had increased from ~2 to ~10 dB. This is in agreement with the decreasing value of δ_{res} from 0.7027 to 0.2440 and the state of resonance is closer to the critical coupling condition.

Immersing MKR in a near-index medium does not always promise an improvement in the resonance condition or RER. There is a possibility that changes in the round-trip attenuation factor and the coupling parameter yield a larger value of δ_{res} and decreases the RER. Figure 5 gives an example for this scenario. The best-fit parameters for $\sin(\kappa l)$ and $\exp(-\alpha L/2)$ are calculated to be 0.6235 and 0.8145, respectively, for immersing the MKR in air, as indicated by the solid curve in Fig. 5. After the MKR was immersed in water (dashed curve), the values of $\sin(\kappa l)$ and $\exp(-\alpha L/2)$ changed to 0.7833 and 0.9339, respectively. Although there was no sign of dust/particle deposited on the microfiber or change in the microfiber knot structure before and after immersion in the water in the observation with an optical microscope, it is believed that the low value of the round-trip attenuation factor can be attributed to the large amount of unseen dust deposited on the microfiber surface when it came into contact with the tweezers during the fabrication of the microfiber knot. After it was immersed in the water, some portion of the deposited dust or particles that were responsible for the scattering loss might have been "washed" away and that increases the round-trip attenuation factor. The decrease in the value of δ_{res} from 0.3881 to 0.5609 is an indication that the resonance condition deviates from critical coupling.

Table 1. Fitting Parameters of the MKR Before and After Immersion in Liquids

	Propan-2-ol		Low-Index Resin		Water	
Parameters	Before	After	Before	After	Before	After
$\sin(\kappa l)$	0.6207	0.6762	0.7132	0.6247	0.6235	0.7833
$\exp(-\alpha L/2)$	0.8547	0.8361	0.9432	0.7538	0.8145	0.9339
δ_{res}	0.5060	0.3679	0.7027	0.2440	0.3881	0.5609
$\alpha\,(\text{m}^{-1})$	170	200	72	347	180	60
$L\,(10^{-3}\,\text{m})$	1.80		1.63		2.28	

Table 1 tabulates all the fitting parameters of the MKR before and after its immersion in different liquid solutions. It is understood that the process of immersion in liquid solution may possibly disturb the structure of the microfiber knot and the output-collector microfiber coupling. A disturbance to the structure in microscale may induce significant influence to the resonance condition of the MKR. Different microfiber waist diameter and orientation of the microfibers in the coupling region have an important relationship with the resonance of the MKR. More investigations pertaining to those parameters are needed. The main focus of this work is to demonstrate the characterization of the MKR resonance condition using the curve-fitting technique.

4. Conclusion

An investigation on the resonance condition of MKR immersed in a solution has been conducted. To assist the analysis, the coupling parameter and the round-trip attenuation factor are obtained by curving fitting the experimental data with a transmission function. The extracted parameters from the best-fit curves provide more quantitative information about the varied resonance condition of an MKR immersed in liquid solutions. In the observation, the coupling coefficient was increased when immersed in liquids. However, depending in the initial state of the coupling and the size of the increment in coupling coefficient when immersed in a liquid, it is possible that the MKR may experience a deficit in the coupling parameter due to the sinusoidal relationship with the coupling coefficient.

This project was funded by the Ministry of Science, Technology and Innovation (MOSTI) under the Brain-Gain Malaysia program.

References

1. K. S. Lim, S. W. Harun, S. S. A. Damanhuri, A. A. Jasim, C. K. Tio, and H. Ahmad, "Current sensor based on microfiber knot resonator," Sens. Actuators A **167**, 60–62 (2011).
2. M. Sumetsky, Y. Dulashko, J. M. Fini, A. Hale, and D. J. DiGiovanni, "The microfiber loop resonator: theory, experiment, and application," J. Lightwave Technol. **24**, 242–250 (2006).
3. Y. Wu, Y.-J. Rao, Y.-H. Chen, and Y. Gong, "Miniature fiber-optic temperature sensors based on silica/polymer microfiber knot resonators," Opt. Express **17**, 18142–18147 (2009).
4. F. Xu, V. Pruneri, V. Finazzi, and G. Brambilla, "An embedded optical nanowire loop resonator refractometric sensor," Opt. Express **16**, 1062–1067 (2008).

5. C. Caspar and E. J. Bachus, "Fibre-optic micro-ring-resonator with 2 mm diameter," Electron. Lett. **25**, 1506–1508 (1989).
6. F. Xu and G. Brambilla, "Embedding optical microfiber coil resonators in Teflon," Opt. Lett. **32**, 2164–2166 (2007).
7. G. Vienne, Y. Li, and L. Tong, "Effect of host polymer on microfiber resonator," IEEE Photon. Technol. Lett. **19**, 1386–1388 (2007).
8. X. Guo, Y. Li, X. Jiang, and L. Tong, "Demonstration of critical coupling in microfiber loops wrapped around a copper rod," Appl. Phys. Lett. **91**, 073512 (2007).
9. F. Bilodeau, K. O. Hill, S. Faucher, and D. C. Johnson, "Low-loss highly overcoupled fused couplers: fabrication and sensitivity to external pressure," J. Lightwave Technol. **6**, 1476–1482 (1988).

seen that for all the considered strip dimensions, all the results are mutually within the 2% deviation, with the most results within 1% deviation only. For $t = w = 0.2$ mm, our results deviate from the exact value of Z_c by less then 1%. This justifies our (and also the others presented) numerical methods.

6. CONCLUSIONS

In this article, strong and weak formulations of higher-order FEM, based on special hierarchical strong and weak basis functions that automatically satisfy the corresponding boundary conditions, are applied for quasi-static solution of shielded planar transmission lines. Applied strong basis functions belong to generalized C^1 continuous functions, they automatically provide the continuity of both potential and the normal component of vector D on interelement boundaries, they are conceptually simple, and they allow simple imposition of boundary conditions (of the first and the second kind) on the outer boundary of the computational domain. Several realistic numerical examples demonstrated accuracy and stability of both FEM formulations. Similar accuracy of both formulations was observed. The weak formulation can handle continuously inhomogeneous elements, but the strong formulation results in less unknowns for the same approximation order.

ACKNOWLEDGMENTS

The presented work is supported by the Serbian Ministry for Science under grants TR-11033 and TR-11021.

REFERENCES

1. J. Jin, The finite element method in electromagnetics, Wiley, New York, 1993.
2. P.P. Silvester, Finite elements for electrical engineers, 3rd ed., Cambridge University Press, Cambridge, England, 1996.
3. V.V. Petrovic and B.D. Popovic, Optimal FEM solutions of one-dimensional EM problems, Int J Numer Modell Electron Networks Devices Field, 14 (2001), 49–68.
4. Available at: http://www.owlnet.rice.edu/~chbe501/Code/Numerical/Library/linbcg.for
5. Z.J. Mancic and V.V. Petrovic, Strong FEM solution for the square coaxial line, Proceedings of TELSIKS 2009 conference, Nis, October 2009, pp 343–346.
6. T.N. Chang and C.H. Tan, Analysis of a shielded microstrip line with finite metallization thickness by the boundary element method, IEEE Trans on MTT, 38 (1990), 1130–1132.
7. Z. Pantic and R. Mittra, Quasi-TEM analysis of microwave transmission lines by the finite-element method, IEEE Trans MTT 34 (1986), 1096–1103.
8. E. Yamashita and K. Atsuki, Analysis of thick-strip transmission lines, IEEE Trans MTT 19 (1971), 120–122.
9. A.R. Djordjevic, M.B. Bazdar, T.K. Sarkar, and R.F. Harrington, Linpar for windows, matrix parameters for multiconductor transmission lines, Software and User's Manual, Artech House, 1996.
10. N.H. Zhu, W. Qiu, E.Y.B. Pun, and P.S. Chung, Quasi-static analysis of shielded microstrip transmission lines with thick electrodes, IEEE Trans MTT 45 (1997), 288–291.
11. S.A. Ivanov and G.L. Djankov, Determination of the characteristic impedance by a step current density approximation, IEEE Trans MTT 32 (1984), 450–452.
12. F. Bowman, Introduction to elliptic functions, English Universities Press, London, Chapter 10, 1953.
13. S.W. Conning, The characteristic impedance of square coaxial line, IEEE Trans MTT 12 (1964), 468–468.

FABRICATION OF MICROFIBER LOOP RESONATOR-BASED COMB FILTER

K. S. Lim,[1] S. W. Harun,[1,2] A. A. Jasim,[2] and H. Ahmad[1]

[1] Department of Physics, Photonics Research Center, University of Malaya, 50603 Kuala Lumpur, Malaysia; Corresponding author: swharun@um.edu.my

[2] Department of Electrical Engineering, Faculty of Engineering, University of Malaya, 50603 Kuala Lumpur, Malaysia

Received 26 July 2010

ABSTRACT: *Microfiber loop resonator (MLR) is fabricated by coiling of a microfiber, which was obtained by the fast stretching of a heated single mode fiber. The MLR is embedded in low refractive index material to keep the system robust. Two comb filters with a constant spacing of 0.16 nm and 0.71 nm are successfully achieved, which the extinction ratio can be adjusted by controlling the state of polarization of the input light. It was also found that the wavelength of each peak and the spacing remain unchanged regardless of the state of polarization of the input light. This MLR does not have major issues with input–output coupling and presents a completely integrated fiberized solution.* © 2011 Wiley Periodicals, Inc. Microwave Opt Technol Lett 53:1119–1121, 2011; View this article online at wileyonlinelibrary.com. DOI 10.1002/mop.25916

Key words: *microfiber; loop resonator; comb filter; fiber tapering*

1. INTRODUCTION

With recent advances in microphotonics and nanophotonics, optical micro- or nanofibers with diameters close to the wavelength of guided light have attracted considerable interest as promising building blocks for a variety of photonic applications [1, 2]. They offer many exciting properties such as large evanescent field, low loss interconnection to other optical fibers and fiberized components, and robustness [1]. In the microfiber device, a considerable fraction of the transmitted power can propagate in the evanescent field outside the microfiber. A micro loop resonator (MLR) can be manufactured by coiling the microfiber on itself. This resonator has been actively researched because of their broad range of applications ranging from optical communications to nonlinear optics, cavity QED, and sensing [2–5]. For instance, Armani et al. [5] recently reported a chemical sensor where label free single molecule detection was achieved in a micro-toroid resonator. Microfiber have been manufactured by using a wide range of techniques: laser ablation [6], electron beam lithography [7], bottom-up methods such as vapor–liquid–solid techniques [8], and top-down techniques such as fiber pulling [9, 10] or direct draw from bulk materials [11]. Among those methods, the flame heating technique has proven to be the most versatile and provides microfiber with the best physical properties [2, 9].

One of the important issues is the comb filtering characteristic of the MLR, which should be adjustable for many applications. In this article, the comb filter construction is demonstrated using the MLR. The effect of the polarization of the input light on the characteristic of the comb filter is investigated. The MLR is fabricated by coiling a microfiber, which was fabricated by drawing of a heated single mode fiber. The device is embedded in low index polymer and sandwiched between two glass substrates to keep the system robust. Because the microfiber is manufactured by adiabatically stretching optical fiber, it maintains the original fiber size at its input and output. This allows a low loss connection via splicing to other optical fibers and fiberized components.

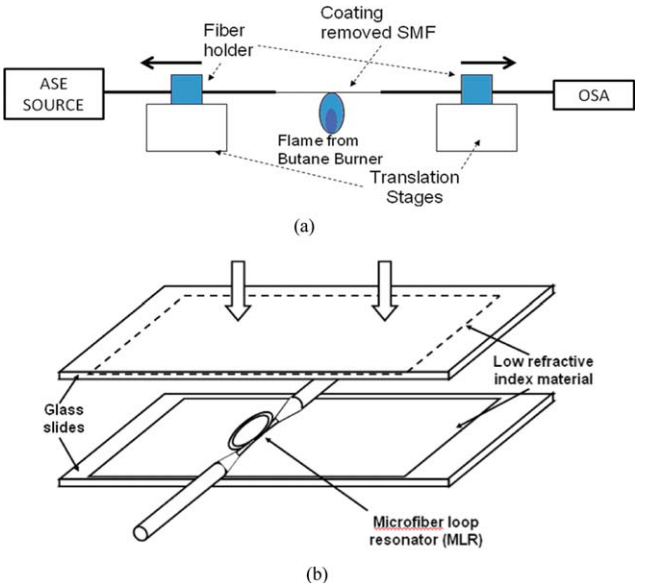

Figure 1 Schematic diagram of experimental set-up for MLR fabrication. (a) Experimental set-up for tapering and coiling a fiber and (b) illustration of MLR embedded in a low refractive index material and sandwiched between two glass plates. [Color figure can be viewed in the online issue, which is available at wileyonlinelibrary.com]

2. FABRICATION AND PACKAGING

A MLR was fabricated using a flame heating method, where the experimental set-up is shown in Figure 1(a). A coating removed standard SMF was held by two fiber holders which were fixed on two translation stages. Both stages have three dimensional translation functions. The fiber ends were connected to an amplified spontaneous emission (ASE) source and an optical spectrum analyzer (OSA). First, a microfiber was fabricated by heating the fiber to its softening temperature and then pulling the ends apart to reduce the fiber's waist diameter down to 1 μm. The heat source is a flame from a butane burner. The flame should be clean, and the burning gas flow should be controlled carefully so that the air convection does not break the fiber during the drawing process. Then, the microfiber is coiled into a self touching loop using two surface attractions, Van der Waals force and electrostatic force, which kept the loop stable because the forces overcame the elastic force to make the fiber straight.

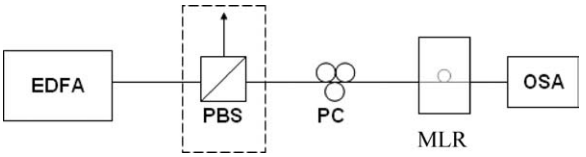

Figure 2 Experimental set-up to investigate the polarization dependent characteristic of the MLR. Polarized wideband source from EDFA is acquired with the aid of PBS (Dashed box), whereas unpolarized wideband source can be obtained by removing PBS from the setup

The fabricated MLR is laid on an earlier prepared glass plate with a thin and flat layer of low refractive index material as shown in Figure 1(b) to address the temporal stability of the device. The thickness of the low refractive index material is $\sim$0.5 mm, which is thick enough to prevent leakage of optical power from the microfiber to the glass plate. Some uncured resin is also applied on surrounding the MLR before it is sandwiched by another glass plate with the same low refractive index resin layer from the top. It is essentially important to ensure that minimum air bubbles and impurity are trapped around the fiber area between the two plates. This is to prevent refractive index nonuniformity in the surrounding of microfiber that may introduce loss to the system. During the tapering, coiling, and coating processes, we monitored both the interference pattern and the insertion loss of the device in real time using the ASE source in conjunction with the OSA. The uncured resin is solidified by the UV light exposure for 3–7 min and the optical properties of the MLR are stabilized.

3. CHARACTERISTIC OF THE COMB FILTER

The microfiber guides light as a single mode waveguide, with the evanescent field extending outside the fiber. This evanescent field depends on the wavelength of operation, on the diameter of the fiber and the surrounding medium. If the microfiber is coiled onto itself, the modes in the two different sections can overlap and couple to create a resonator with an extremely compact geometry. In the MLR, the input light is allowed to oscillate in the loop and the resonance is strongest when a positive interference

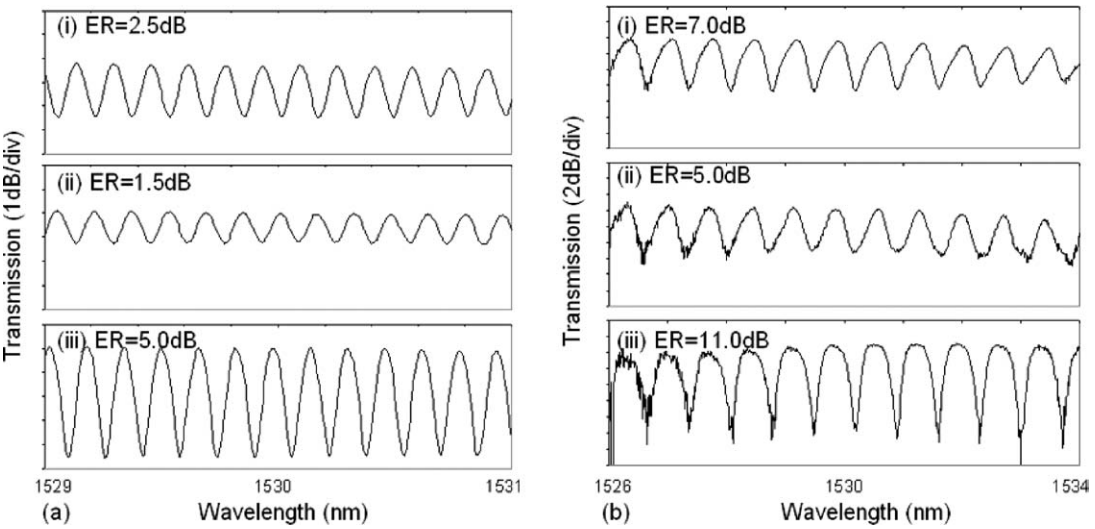

Figure 3 The output comb spectra from two different MLRs with (a) FSR = 0.16 nm and (b) FSR = 0.71 nm for different input signal state of polarizations

condition is fulfilled. The MLR can be fabricated depending on the desired free spectral range (FSR) or spacing of the comb filter by controlling the loop length, L parameter according to the following well known equation.

$$\mathrm{FSR} = \lambda^2 / n_g L$$

where λ is the wavelength, n_g is the group index of the mode propagating in the microfiber. The main focus of this study is to investigate how the changes of input polarization state affect the characteristic of the comb filter.

Figure 2 shows the experimental set-up to investigate the polarization dependent characteristic of the fabricated MLR. An unpolarized ASE source from an Erbium-doped fiber amplifier (EDFA) is linearly polarized by a polarizing beam-splitter (PBS) before it is launched into the fabricated MLR. A polarization controller (PC), which is located in between the source and MLR, is used to control the state of polarization of the light source. The output spectrum from the MLR is characterized by an OSA. The experiment is also repeated using an unpolarized input wave, which was obtained by removing PBS from the set-up for comparison purpose. Figure 3 shows the transmission spectra of fabricated MLRs under three different scenarios; (i) without PBS, (ii) with PBS and PC is adjusted to obtain the smallest extinction ratio, and (iii) with PBS and PC is adjusted to obtain the highest extinction ratio. Figures 3(a) and 3(b) show the spectra obtained from the MLRs, which were designed to achieve FSR of 0.16 and 0.71, respectively. Since both transmission spectra of (i) in Figure 3 were acquired based on an unpolarized input light and the resonating condition is found to be unaffected by the adjustment of the PC. In contrast, the resonating condition for the MLR with polarized input light is very sensitive to the PC adjustment as illustrated in spectra (ii) and (iii) of Figure 3. The transmission spectra (ii) and (iii) show the smallest and the highest resonance extinction ratio respectively, which were achieved by a polarized input light with careful adjustment of PC.

As seen in Figure 3, it was found that the wavelength of each peak and the FSR remain unchanged regardless of the state of polarization of the input light. The change of the extinction ratio as a consequence of polarization state can be explained by a change in coupling condition between tapered microfibers. The coupling condition changes with the refractive index of the microfiber, which depends on the birefringence. The coupling efficiency at the self touching part of the microfiber can be manipulated by the adjustment of PC and subsequently changing the resonating condition of the MLR. These results show that the extinction ratio of the MLR can be improved by using an optimized polarized input light. This property may be useful in many applications such as multiwavelength laser generation and sensing.

4. CONCLUSIONS

Two MLR-based comb filters with FSRs of 0.16 and 0.71 were successfully fabricated, and their polarization dependent characteristic has been demonstrated. Both MLRs are fabricated by coiling a microfiber on itself and keeping two sections of a microfiber together by taking advantage of surface attraction forces. The fabricated MLR is embedded in a low refractive index material to improve its stability and robustness. The extinction ratio of the comb filter can be adjusted by controlling the state of polarization of the input light. It was also found that the wavelength of each peak and the FSR remain unchanged regardless of the state of polarization of the input light.

REFERENCES

1. G. Brambilla, Y. Jung, and F. Renna, Optical fiber microwires and nanowires manufactured by modified flame brushing technique: Properties and applications, Front Optoelectron China 3 (2010), 61–66.
2. S.W. Harun, K.S. Lim, A.A. Jasim, and H. Ahmad, Fabrication of tapered fiber based ring resonator, Laser Phys 7 (2010).
3. F. Xu and G. Brambilla, Demonstration of a refractometric sensor based on optical microfiber coil resonator, Appl Phys Lett 92 (2008), 101126.
4. X. Jiang, Y. Chen, G. Vienne, and L. Tong, All-fiber add-drop filters based on microfiber knot resonators, Opt Lett 32 (2007), 1710–1712.
5. A.M. Armani, R.P. Kulkarni, S.E. Fraser, R.C. Flagan, and K.J. Vahala, Label-free, single-molecule detection with optical microcavities, Science 317 (2007), 783–787.
6. A.M. Morales and C.M. Lieber, A laser ablation method for the synthesis of crystalline semiconductor nanowires, Science 279 (1998), 208–211.
7. J. Chen, M.A. Reed, A.M. Rawlett, and J.M. Tour, Large on-off ratios and negative differential resistance in a molecular electronic device, Science 286 (1999), 1550–1552.
8. J. Westwater, D.P. Gosain, S. Tomiya, S. Usui, and H. Ruda, Catalytic growth of silicon nanowires via gold/silane vapor-liquid-solid reaction, J Vac Sci Technol B 15 (1997), 554–557.
9. G. Brambilla, V. Finazzi, and D.J. Richardson, Ultra-low-loss optical fiber nanotapers, Opt Express 12 (2004), 2258–2263.
10. A.M. Clohessy, N. Healy, D.F. Murphy, and C.D. Hussey, Short low-loss nanowire tapers on singlemode fibres, Electron Lett 41 (2005), 27–29.
11. X. Xing, Y. Wang, and B. Li, Nanofibers drawing and nanodevices assembly in polytrimethylene terephthalate, Opt Express 16 (2008), 10815–10822.

NOVEL DESIGN OF AN ULTRA-WIDEBAND MICROSTRIP ANTENNA EMPLOYING A LOBSTER-SHAPED RESONANT STRUCTURE

A. Abbaspour,[1] Mohammad Naser-Moghadasi,[2] and Morteza Katouli[2]
[1] Department of E & E Engineering, Sharif University, Tehran, Iran
[2] Faculty of Engineering, Science and Research Branch, Islamic Azad University, Tehran, Iran; Corresponding author: mn.moghaddasi@srbiau.ac.ir

Received 28 July 2010

ABSTRACT: *In this article, a microstrip-fed planar monopole antenna incorporating a lobster-shaped resonant structure, which is etched on its back plane is presented. Simulated Impedance bandwidth of the proposed antenna is ~115% over an ultra-wideband frequency range between 3 and 11.2 GHz satisfying FCC's frequency band.* © 2011 Wiley Periodicals, Inc. Microwave Opt Technol Lett 53:1121–1125, 2011; View this article online at wileyonlinelibrary.com. DOI 10.1002/mop.25925

Key words: *microstrip-fed planar antenna; ultra wideband; resonant structure*

1. INTRODUCTION

Ultra-wideband (UWB) technology has been used in the areas of radar, sensing, and military communications during the past two decades. A substantial surge of research interest has occurred since February 2002, when the FCC issued a ruling

Published in IET Optoelectronics
Received on 13th January 2011
Revised on 17th May 2011
doi: 10.1049/iet-opt.2011.0008

ISSN 1751-8768

Low-cost spectral tunable microfibre knot resonator

K.S. Lim[1] S.W. Harun[1,2] S.S.A. Damanhuri[2] A.A. Jasim[2] H.H. Ku[2] H. Ahmad[1]

[1]Photonics Research Center, Department of Physics, University of Malaya, Kuala Lumpur 50603, Malaysia
[2]Department of Electrical Engineering, University of Malaya, Kuala Lumpur 50603, Malaysia
E-mail: swharun@um.edu.my

Abstract: A low-cost microfibre knot resonator (MKR) is fabricated and the resonant wavelength tunability characteristic of this device is investigated and demonstrated. The spacing of the transmission comb spectrum is unchanged with the temperature, but the resonant wavelength linearly shifts with the temperature change at a slope coefficient of 50.6 pm/°C. The resonant wavelength can also be tuned by applying electric current to the copper wire, which is fastened by the microfibre knot. This is attributed to the thermally induced optical phase shift in the MKR caused by the heat produced by the flow of the electric current over a short transit length. The authors' analysis indicates that the wavelength shift is linearly proportional to square of the current and the maximum tuning slope achieved is 51.3 pm/A^2.

1 Introduction

Optical microfibres are optical fibres with diameters close to the wavelength of the guided light. It has a number of interesting optical properties such as tight optical confinement, large evanescent fields, strong field enhancement and large waveguide dispersions [1–3], which offer plenty of opportunities for developing microphotonic or nanophotonic components/devices ranging from interferometers, filters, lasers and sensors. To date, several microfibre fabrication techniques have been developed such as the flame brushing technique [4], indirect flame heating [5], CO_2 laser [6] and electric microheater [7]. The fabricated microfibres are used in producing many photonic structures such as loop resonator, coil resonator, knot resonator, Sagnac interferometer and so on [8, 9].

Owing to the large evanescent field of the microfibres, microfibre devices are sensitive to the ambient condition. Thus, microfibre optical resonators are recommended in many sensing applications particularly in the chemical, refractive index and temperature sensing [10–12]. In the case of temperature sensing, the transmission spectrum of the microfibre-based resonator shifts as the ambient temperature varies. This is owing to the thermal dependency of the microfibre length and refractive index [12]. In reciprocal, the transmission spectrum of the resonator can be tuned by manipulating the temperature of the resonator. In this paper, a new microfibre knot resonator (MKR) is fabricated by wrapping a microfibre on a copper wire. Spectral tunability is then demonstrated in the fabricated MKR based on the idea of thermally induced resonant wavelength shift. A microfibre knot is formed tightly around a copper wire and the electric current that passes through the copper wire is varied such that the copper wire acts as a heating element and induces temperature change in the MKR. The transmission spectrum of the MKR shifts corresponds to the temperature change. These modified MKRs can be used as low-cost and fast response tunable optical filters, which are useful in the applications of optical signal processing, wavelength division multiplexing communication and so on.

2 Theoretical analysis on temperature response on MKR

MKRs exhibit similar optical properties as microfibre loop resonators, where the free spectral range (FSR) of the device takes the form of [3]

$$\mathrm{FSR} \simeq \frac{\lambda^2}{n_{\mathrm{eff}} L} \tag{1}$$

where λ is the wavelength, n_{eff} is the effective index of the microfibre and L denotes the single roundtrip length in the resonator. The temperature variation of the MKR is an important factor, which affects the n_{eff} and the loop length L of the microfibre knot. These variations may lead to transmission spectral shift and the relationship can be expressed as

$$\frac{\Delta\lambda_{\mathrm{res}}}{\lambda_{\mathrm{res}}} = \left(\frac{\Delta n_{\mathrm{eff}}}{n_{\mathrm{eff}}} + \frac{\Delta L}{L}\right)_{\mathrm{Temp}} \tag{2}$$

In relation with temperature, both terms on the right side of (2) can be well expressed as two linear thermal equations with thermal-optic coefficient (TOC) and thermal expansion coefficient (TEC) as shown below [12].

$$\frac{\Delta n_{\mathrm{eff}}}{n_{\mathrm{eff}}} = \alpha_{\mathrm{TOC}} \Delta T \tag{3a}$$

$$\frac{\Delta L}{L} = \alpha_{\mathrm{TEC}} \Delta T \tag{3b}$$

Substitution of (3a) and (3b) into (2) produces

$$\frac{\Delta\lambda_{res}}{\lambda_{res}} = (\alpha_{TOC} + \alpha_{TEC})\Delta T \quad (4)$$

3 Experimental setup

At first, a microfibre is fabricated from a silica-based single mode fibre (SMF) using a flame-brushing method. After removing the polymer protective cladding from a piece of SMF, a microfibre is made by heating and stretching the SMF until the waist diameter is reduced to ~2 μm. Then the microfibre is cut and separated into two unequal parts in which the longer one is used in the knot fabrication and the other part is used as a collector fibre to collect the transmitted light from the MKR [3]. The microfibre knot is assembled by micromanipulating the longer part of the microfibre, which has a high diameter uniformity and excellent sidewall smoothness. The microfibre is first twisted into a relatively large loop, which is slightly larger than the diameter of the copper wire. The copper wire is inserted into the microfibre loop so that it can be tightened onto the copper wire by pulling the free ends of the fibre as illustrated in Fig. 1. The other part of microfibre (the collector microfibre) is used to collect the light transmitted out from the knot by means of evanescent coupling. At least ~3 mm of coupling length between the two microfibres is required to achieve strong van der Waal attraction force to keep them attached together as shown in Fig. 1. The wire diameter is measured to be ~185 μm. Copper has negligibly small thermal expansion coefficient (17×10^{-6}/°C), as long as the wrapped knot diameter is not made very tight on the copper wire. There is enough room for the expansion of heated wire.

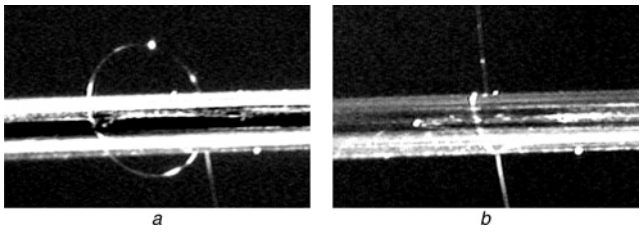

Fig. 1 *Optical microscope image of MKR with a copper wire inserted into the knot*

a Before tightening by pulling both ends of the microfibre
b After tightening by pulling both ends of the microfibre

The optical characteristics of the resonator are strongly affected by the tensile strain on the microfibre arms of the MKR because of the pulling on the microfibre arms. It is essential to reduce the tension on both arms of the MKR by moving the fibre holders a bit closer to the microfibre knot after the knot is fastened. However, the movement causes very little change in the knot diameter and the resonance condition of the MKR remains good and stable after the tension is lessened. The comb transmission spectrum characteristic of the MKR is measured using an amplified spontaneous emission source in conjunction with an optical spectrum analyser (OSA). The MKR is then placed in an oven with temperature control to investigate how the comb spectrum changes with the temperature.

4 Results and discussion

Fig. 2 shows the transmission spectra of the MKR at temperatures of 30, 35 and 40°C. As shown in the figure, the spacing of the transmission comb spectrum is unchanged with temperature, but the spectrum is shifted at ~26 pm for every temperature increment of 5°C. The change of temperature not only affects the resonance condition of the microfibre knot, but also affecting the coupling between the fibre end of the knot resonator and collector microfibre. As a consequence, the coupling efficiency at the collection fibre and transmission power varies with the change of temperature.

Fig. 3 shows the resonant wavelength shift with the temperature change, which demonstrates a linear trend with a spectral sensitivity of 50.6 pm/°C. As for the case of MKR-tied copper wire, the copper wire acts as a heating element when current is flowing in it. The dissipated heat contributes to the instantaneous temperature rise in the MKR. Considering the linear relationship between the temperature change and heat energy generated by the conducting current, the relationship between the wavelength shift and the conducting current I assumes the form of

$$\frac{\Delta\lambda_{res}}{\lambda_{res}} \propto \frac{\rho I^2}{A} \quad (5)$$

where ρ and A represent the conductor resistivity and the cross-sectional area of the conductor rod, respectively. The term ρ/A in (5) is equivalent to resistance per unit length of

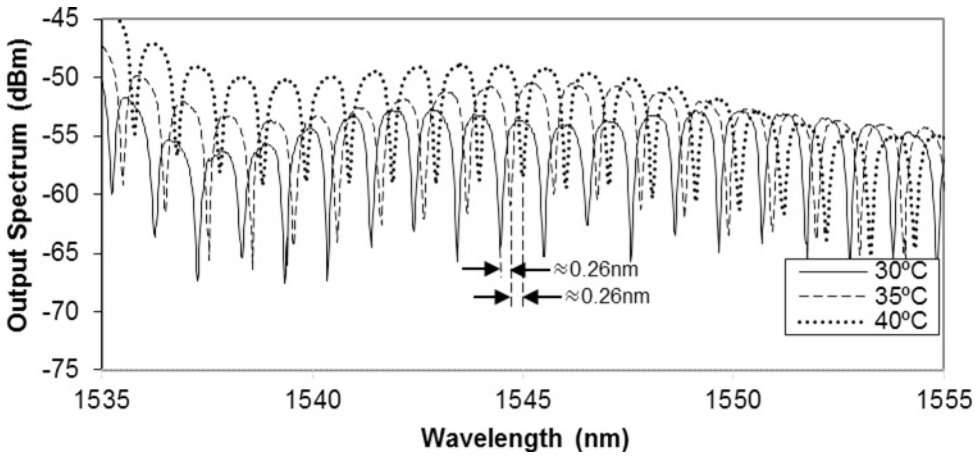

Fig. 2 *Output spectra of an MKR at temperature of 30°C (solid), 35°C (dashed) and 40°C (dotted)*

doi: 10.1049/iet-opt.2011.0008

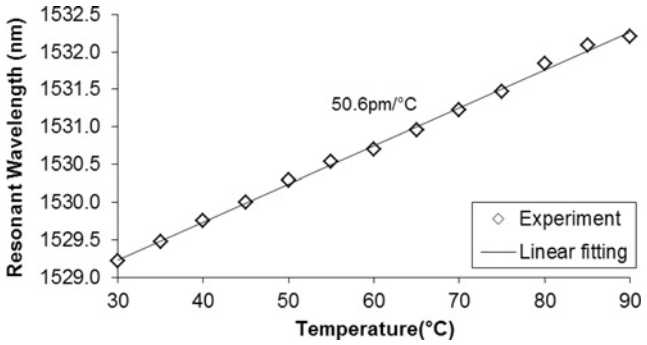

Fig. 3 *Temperature response of the MKR displays spectral sensitivity of 50.6 pm/°C*

the conductor material. The resistivity of the copper wire is $1.68 \times 10^{-8}\ \Omega$ m.

Fig. 4 shows the resonant spectra of the MKR with a copper wire with different currents. In the experiment, the applied current is uniformly increased from 0 to 2 A. As shown in Fig. 4, the resonant wavelength shifts to a longer wavelength with the increase in the conducting current of the copper wire. This is the result of increase temperature in the MKR. From the observation on the OSA, the measured response time of the wavelength shift is ~3 s and the spectrum comes to a steady condition after 8 s. Therefore each spectrum is recorded at ~10 s after the copper wire is loaded with an electric current. As the source of heat, the peak temperature is at the wire and the closer the microfibre knot to the wire, the shorter the response time. At current $I = 1.0$ A, the resonant wavelength is shifted by ~30 pm from 1530.56 to 1530.59 nm and at $I = 2.0$ A, the resonant wavelength is further shifted to 1530.77 nm, 210 pm from the original wavelength. It is also observed that the transmission spectrum always shifts toward the longer wavelength direction with increasing current regardless of the current flow direction, and the spectrum returns to the original state once current supply is terminated. Fig. 4 presents no sign of power fluctuation like the one shown in Fig. 2 because the evanescent coupler, that is, responsible the power fluctuation is far from the heat source (copper wire).

The experiment is also repeated using two copper wires for comparison purpose. In this case, the MKR is tightened onto two copper wires with an identical wire diameter. The measured FSR and knot diameter of the single wire MKR are 1.7 nm and ~317 μm, respectively, whereas for the two wires MKR, the measured FSR and knot diameter are 1.46 nm and ~370 μm. An alternating current flows through the copper wire and the resonant wavelength shift is investigated against the applied current for both cases; single and two wires arrangements. At a small current of <0.5 A, no significant resonant wavelength shift is observed. Starting from 0.6 A, the resonant wavelength shifts gradually move toward the longer wavelength. At the maximum current of 2.0 A (or $I^2 = 4.0\ \text{A}^2$), a wavelength shift of 0.21 and 0.09 nm are achieved with single and two copper wires arrangements, respectively. Fig. 5 shows the resonant wavelength shift against the square of the current (I^2) for both cases. The data set of each configuration can be well fitted to a linear regression line with a correlation coefficient value of $r > 0.95$. This justifies the linear relationship stated in (5). The cross-sectional area of the wire of the MKR with two wires is twice as large as the single-wire configuration. Based on the relationship in (5), the tuning slope of the wavelength shift against I^2 of the MKR with two wires should be half of that of the single wire. However, the experimental result of Fig. 5 shows that the slope of MKR with single and two wires are obtained at 51.3 and 19.5 pm/A^2, respectively. The discrepancy between the analysis and experimental outcomes is most probably because of the difference in the orientation and position of the wire(s) in the MKR. The calculated temperature-to-square-current slopes of the single-wire and two-wire MKR are 1.01 and 0.385°C/A^2, respectively. As the source of heat, the temperature of the copper wire should be slightly higher than that of MKR but not far from it because of the close proximity between the microfibre and wire. At $I = 2$ A, the estimated minimum temperatures of the single copper wire and two copper wire are 32 and 29.5°C, respectively, assuming that the room temperature is 28°C. The tuning slope and dynamic range of the modified MKR can be further improved by using different conductors with higher resistivity such as nichrome, constantan, graphite and so on, which are commonly used as heating elements. Conductor with high resistivity may help reducing the operating current for the proposed filter. However, the suitability of the elements when integrated with the microfibre or other opto-dielectric device requires further investigation. The coupling between knot resonator output and collector microfibre is highly dependent on temperature. The output power of the MKR can be unstable in a varying temperature environment. Temperature control could help solving this problem.

The simple fabrication technique and abundant raw materials enable low-cost fabrication of the proposed comb filter. This filter has a micrometer scale dimension and it is compatible with the standard fibres and other optical components. Further investigation on the filter based on the transfer function of MKR is in progress.

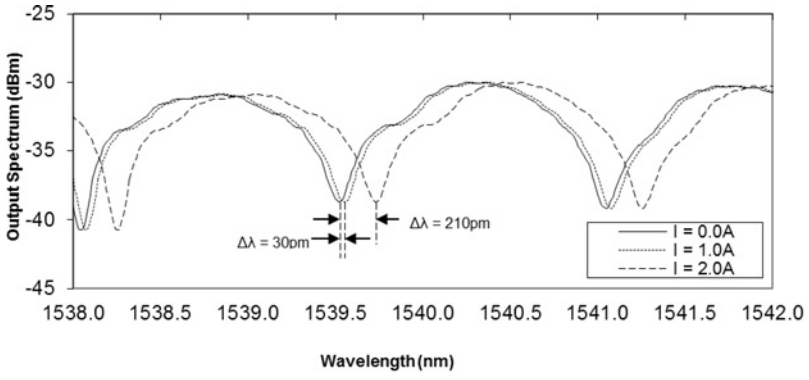

Fig. 4 *Transmission spectra of the MKR with a single copper wire at different current*

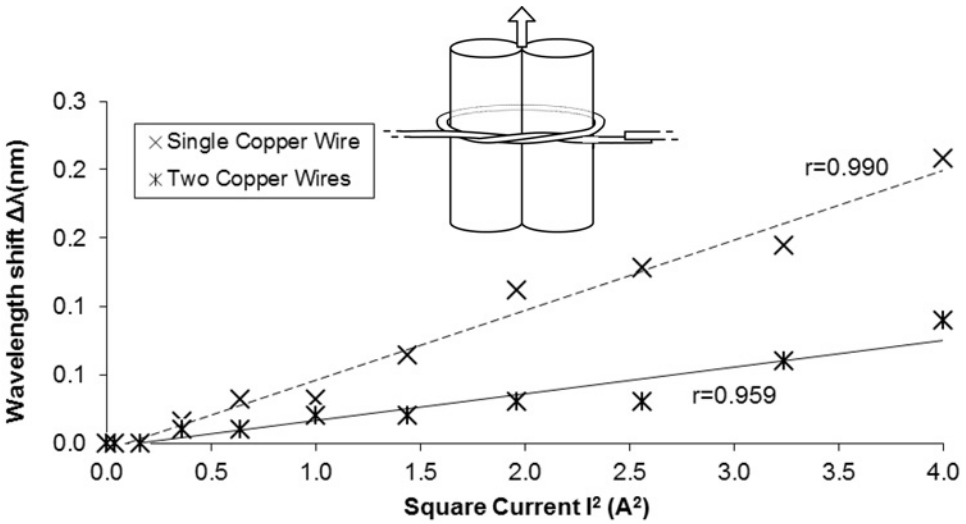

Fig. 5 *Wavelength shift against the squared value of the injected current for both MKRs with single and two wire arrangements*

Calculated resistance of the single copper wire and two copper wire are 0.53 and 0.26 $\Omega\ m^{-1}$, respectively. Inset shows the schematic illustrations of MKR with two copper wires

5 Conclusion

A low-cost spectral tunable MKR-based comb filter is proposed by exploiting the thermal dependency of the microfibre length and the refractive index of the MKR. The spacing of the transmission comb spectrum is observed to be linearly shifted with the temperature change at the slope coefficient of 50.6 pm/°C. This resonant wavelength shift can also be achieved by applying electric current through the copper wire to heat up the MKR wrapped around it. The theoretical and experimental analysis suggests that the tuning slope of the modified MKR can be manipulated by using different cross-sectional area and resistivity of the conductor wire. Experimentally, a tuning slope of 51.3 pm/A^2 based on single copper wire configuration has been demonstrated.

6 References

1 Birks, T.A., Li, Y.W.: 'The shape of fiber tapers', *J. Lightwave Technol.*, 1992, **10**, (4), pp. 432–438

2 Harun, S.W., Lim, K.S., Jasim, A.A., Ahmad, H.: 'Dual wavelength erbium-doped fiber laser using a tapered fiber', *J. Mod. Opt.*, 2010, **57**, pp. 2111–2113

3 Sumetsky, M., Dulashko, Y., Fini, J.M., Hale, A., DiGiovanni, D.J.: 'The microfiber loop resonator: theory, experiment, and application', *J. Lightwave Technol.*, 2006, **24**, (1), pp. 242–250

4 Harun, S.W., Lim, K.S., Jasim, A.A., Ahmad, H.: 'Fabrication of tapered fiber based ring resonator', *Laser Phys.*, 2010, **20**, (7), pp. 1629–1631

5 Tong, L., Gattass, R.R., Ashcom, J.B., *et al.*: 'Subwavelength-diameter silica wires for low-loss optical wave guiding', *Nature*, 2003, **426**, pp. 816–819

6 Kakarantzas, G., Dimmick, T.E., Birks, T.A., Le Roux, R., Russell, P.St.J.: 'Miniature all-fiber devices based on CO_2 laser microstructuring of tapered fibers', *Opt. Lett.*, 2001, **26**, (15), pp. 1137–1139

7 Brambilla, G., Koizumi, F., Feng, X., Richardson, D.J.: 'Compound-glass optical nanowires', *Electron. Lett.*, 2005, **41**, (7), pp. 400–402

8 Sumetsky, M.: 'Basic elements for microfiber photonics: micro/nanofibers and microfiber coil resonators', *J. Lightwave Technol.*, 2008, **26**, (1), pp. 21–27

9 Jiang, X., Tong, L., Vienne, G., *et al.*: 'Demonstration of optical microfiber knot resonators', *Appl. Phys. Lett.*, 2006, **88**, (22), p. 223501

10 Xu, F., Horak, P., Brambilla, G.: 'Optical microfiber coil resonator refractometric sensor', *Opt. Express*, 2007, **15**, (12), pp. 7888–7893

11 Sumetsky, M., Windeler, R.S., Dulashko, Y., Fan, X.: 'Optical liquid ring resonator sensor', *Opt. Express*, 2007, **15**, (22), pp. 14376–14381

12 Zeng, X., Wu, Y., Hou, C., Baia, J., Yang, G.: 'A temperature sensor based on optical microfiber knot resonator', *Opt. Commun.*, 2009, **282**, (18), pp. 3817–3819

doi: 10.1049/iet-opt.2011.0008